Application of Shack-Hartmann wavefront sensing technology to transmissive optic metrology

R. R. Rammage, D. R. Neal, and R. J. Copland; WaveFront Sciences Inc.

ABSTRACT

Human vision correction optics must be produced in quantity to be economical. At the same time every human eye is unique and requires a custom corrective solution. For this reason the vision industries need fast, versatile and accurate methodologies for characterizing optics for production and research. Current methods for measuring these optics generally yield a cubic spline taken from less than 10 points across the surface of the lens. As corrective optics have grown in complexity this has become inadequate. The Shack-Hartmann wavefront sensor is a device that measures phase and irradiance of light in a single snapshot using geometric properties of light. Advantages of the Shack-Hartmann sensor include small size, ruggedness, accuracy, and vibration insensitivity. This paper discusses a methodology for designing instruments based on Shack-Hartmann sensors. The method is then applied to the development of an instrument for accurate measurement of transmissive optics such as gradient bifocal spectacle lenses, progressive addition bifocal lenses, intraocular devices, contact lenses, and human corneal tissue. In addition, this instrument may be configured to provide hundreds of points across the surface of the lens giving improved spatial resolution. Methods are explored for extending the dynamic range and accuracy to meet the expanding needs of the ophthalmic and optometric industries. Data is presented demonstrating the accuracy and repeatability of this technique for the target optics.

Keywords: Aberrometer, Transmissive Optics Tester, Shack-Hartmann sensor, wavefront sensor, lens testing, Intraocular lens testing, Contact lens testing, Hartmann Shack sensor

1. INTRODUCTION

A light wavefront may be defined as the virtual surface defined by the point on all possible rays having equal optical path length from a spatially coherent source. The wavefront of light emanating from a point light source is a sphere. The wavefront created by an ideal collimating lens mounted at its focal length from a point source is a plane. A wavefront sensor may be used to test the quality of a transmissive optics system, such as a collimating lens, by detecting the wavefront emerging from the system and comparing it to some expected ideal wavefront. Such ideal wavefronts may be planar, spherical, or have some arbitrary shape dictated by other elements of the optical system. The optical system might be a single component or may be very complex.

A Shack-Hartmann Wavefront Sensor is a device that uses the fact that light travels in a straight line to measure the wavefront of light. The device consists of a lenslet array that breaks an incoming beam into multiple focal spots falling on a optical detector as illustrated in Figure 1. By sensing the position of the focal spots the propagation vector of the sampled light can be calculated for each lenslet. The wavefront can be reconstructed from these vectors.   Shack-Hartmann sensors have a finite dynamic range determined by the need to associate a specific focal spot to the lenslet it represents. A typical methodology for accomplishing this is to divide the detector surface into regions (Areas-of-Interest or AOI's) where the focal spot for a given lenslet is expected to fall. If the wavefront is sufficiently aberrated to cause the focal spot to fall outside
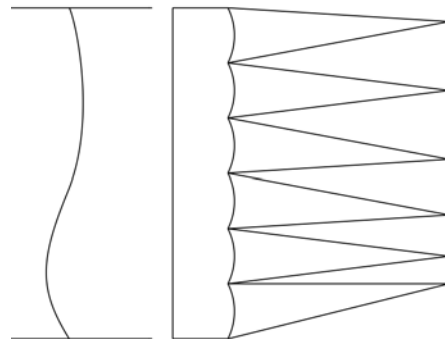

Figure 1. Shack-Hartmann Sensor

this region or not be formed at all, the wavefront is said to be out of the dynamic range of the sensor. In practice these sensors have a much greater dynamic range than Interferometric Sensors. This range may be tens to hundreds of waves of optical path difference.
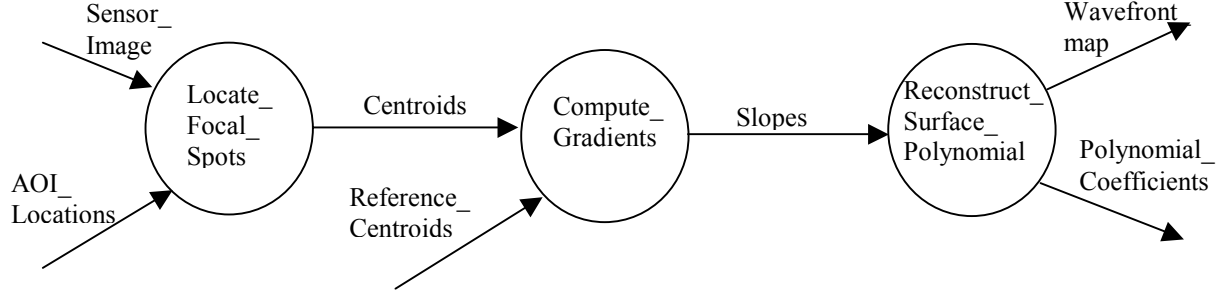
Wavefront Analysis

Figure 2. Data Flow Diagram of Wavefront Analysis Train

For a detailed discussion of the analysis train see Neal, Copland and Roller[1]. For the purpose of this paper it is important to understand the computation at only a very high level.

Locate_Focal_Spots – this process implements some algorithm such as a Center-of-Mass computation that locates the central tendency of each focal spot. A Centroid (ρ) consists of an X and a Y position and for the Center-of-Mass algorithm may be expressed as:

$$\rho_l^x = \frac{\sum_{i=W_l^x}^{W_{l+1}^x} \sum_{j=W_l^y}^{W_{l+1}^y} I_{ij} x_i}{\sum_{i=W_l^x}^{W_{l+1}^x} \sum_{j=W_l^y}^{W_{l+1}^y} I_{ij}} \ and \ \rho_l^y = \frac{\sum_{i=W_l^x}^{W_{l+1}^x} \sum_{j=W_l^y}^{W_{l+1}^y} I_{ij} y_j}{\sum_{i=W_l^x}^{W_{l+1}^x} \sum_{j=W_l^y}^{W_{l+1}^y} I_{ij}} \qquad \text{Equation 1.}$$

where I is the pixel brightness, x and y are pixel coordinates, and W represents the AOI boundries for a given AOI l.

Compute_Gradients – this process computes the Slope information for each lenslet. The average slope or gradient over a given lenslet is simply the difference between the measurement Centroid locations and those of a Reference Centroid taken earlier.

$$\left(\frac{\partial \varphi}{\partial x}\right)_l = \frac{\rho_l^x - \rho_{l,ref}^x}{f} \ and \ \left(\frac{\partial \varphi}{\partial y}\right)_l = \frac{\rho_l^y - \rho_{l,ref}^y}{f} \qquad \text{Equation 2.}$$

where f is the focal length of the lenslet array and ρ represents Centroid coordinates for both measurement and reference of a given lenslet or AOI l.

Reconstruct_Surface_Polynomial – this process infers the wavefront surface from the measured gradients by some algorithm such as a Least-Squares Fit of the gradients to the derivative of a polynomial. The most commonly used polynomial is the Zernike polynomial. A number of other useful polynomial possibilities include Chebyshev, Laguerre, Hermite-Gaussian, or Taylor. The polynomial may be evaluated to provide a wavefront map or this may be computed by integrating the slopes across the measurement aperture.

Data Presentation Format

The output from a wavefront sensor is normally a wavefront map. The wavefront at each point in the pupil is referenced to an ideal spherical wave and deviations from the sphere are the wavefront error. A region that has a deviation from the spherical wave corresponds to reduced resolution and degraded optical quality. The larger the deviation is, the more the degradation. If the wavefront map has been printed in color, it is very easy to identify regions that degrade the image just by looking for the regions that have colors toward the minimum or maximum of the color scale.

Unfortunately, the wavefront map concept is generally unfamiliar to ophthalmologists and optometrists. Instead, a concept that they are more comfortable with is the power map since those have been made available as an output from corneal topographers since the mid-1990s.

Power is a well defined optical quantity for a spherical surface,

$$p = \frac{(n_1 - n_2)}{r} \qquad\qquad \text{Equation 3.}$$

where r is the radius of curvature of the refracting surface and n_1 and n_2 are the refractive indices of the media. When r is in meters, p is in Diopters. Of course perfect spheres are not of much interest so the concept of power has been variously extended to describe more complicated refracting surfaces.

One variation of a power map is known as an "axial power map." Consider a rotationally symmetric refracting surface and a bundle of collimated rays traveling along the optical axis. The rays are bent by the refracting surface and then cross the optical axis at some distance behind the vertex of the surface. The distance each ray crosses the axis from the vertex then would be related to the surface power. So each location on the surface can be assigned a power.

If the surface is not rotationally symmetric, the utility of the axial power map breaks down. If the surface has astigmatism or other aberration, most of the rays will be skew and never intersect the optical axis. Variations of the power map that can deal with non-rotationally symmetric surfaces are called "true power maps," "tangential power maps" or "instantaneous power maps."

All the power map concepts suffer from a common flaw. The focusing power of a region is of interest obviously. But the direction of the light is just as important. Regions on a power map that have the same power may actually focus the light at different areas and cause badly degraded images. And regions of the optic that have different powers may actually be sending the light to the same focal area, thus actually making a fairly good image. For this reason, power maps are inherently flawed. Wavefront maps are much more useful. For these reasons we chose not to use power map as an output format for this study. Power map displays will be included in the final product shipped to customers.

2. TRANSMISSIVE OPTICS TESTER ARCHITECTURE

A transmissive optics test instrument may be designed by selection and design of four functional subcomponents. These subcomponents are illustrated in Figure 3. For an additional discussion of wavefront sensor instrument design see Neal, Armstrong, and Turner[2]. In the description below, each functional element is examined in the correct order of consideration.

FIGURE 3. FUNCTIONAL BLOCK DIAGRAM
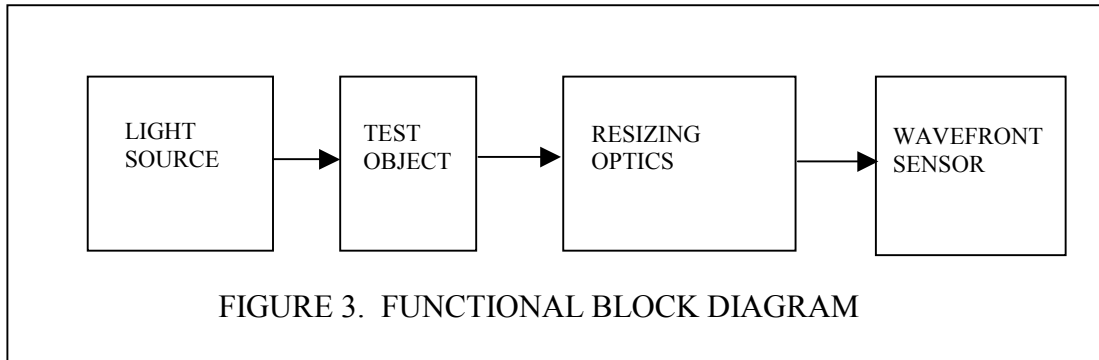
Test Object
Several characteristics of the Test Object must be considered before designing the other components of the instrument. These are: 1) Mounting and control requirements for the test optic; 2) Diameter of the test optic; and 3) Expected Aberration range for the test optic. For many of the Ophthalmic Optics that were the target of the present instrument, the optic must be measured underwater or in a saline solution. Contact lenses in particular are made very thin hydrous material and deform under their own weight if the measurement cell is in a vertical orientation. These measurements must be made in a specially constructed wet cell designed to allow the lens to float in saline solution while still controlling the position in the measurement aperture. Spectacle lenses are much larger and are irregularly shaped and so have their own special requirements for mounting and control.

Light Source
Coherence – The Shack – Hartmann wavefront sensor does not require a temporally coherent light source. It does, however require a light source that is spatially coherent. This means that it is possible to use a collimated or point "white" light source.

Power – Sufficient light must fall on the wavefront sensor to provide focal spots where the brightest pixel is between 50% and 90% of the camera range. Most of these sensors are based on standard machine vision or scientific grade CCD cameras. Because the light falling on a given lenslet is focused into focal spot smaller than the lenslet itself, there is a light gathering or concentration effect. The result is that very little light is needed to make a measurement. More often the need is to reduce or attenuate the light falling on the sensor rather than increase it. Attenuation, must be accomplished in a way that does not introduce unnecessary aberrations into the optical system.

Wavelength – Wavelength is often the prime consideration in the choice of a light source. Often an optic is intended to be used at a specific wavelength and therefore must be tested at that wavelength. If chromatic aberration is a concern it may be important to test the optic over a large range of wavelengths. The reason for considering the light source before determining the other functional components is that this decision impacts all the other choices such as the type of wavefront sensor camera, choice of optic coatings in the resizing optics and so on.

Wavefront Sensor
Five requirements are considered for selecting a wavefront sensor. They are wavelength, spatial resolution, sensitivity, dynamic range, and signal-to-noise performance. All four are interrelated in the design of the sensor, causing trade-offs. Therefore, they must be considered together.

Table 1. Off-the-Shelf Wavefront Sensor Options

Diameter	Focal Length	Array Size	Sensitivity	Dynamic Range
252 μm	25 mm	25 x 19	λ / 150	30 λ
198 μm	15.5 mm	31 x 24	λ / 100	40 λ
144 μm	8 mm	44 x 33	λ / 50	50 λ
108 μm	4.6 mm	58 x 44	λ / 30	70 λ
72 μm	2 mm	88 x 66	λ / 10	120 λ

Wavelength – The wavelength of a measurement determines the sensor technology used for the wavefront sensor camera. For measurements in the long UV region (below 340 nm), Lumogen coated CCD's are used. Bare CCD's work well for the visible wavelengths up to 1.0 μm. In the near IR region InGaAS arrays are used. Each of these technologies have different possibilities for the size of pixel that can be created on the sensor chip. Since focal spot location is a statistical process and smaller pixels result in more pixels on the CCD detecting a portion of a given focal spot, smaller pixels result in better sensitivity and Signal-to-noise performance for a given sensor. Visible range CCD's generally have the smallest pixel size.

Spatial Resolution – The spatial resolution is simply the diameter of the subaperture or lenslet that is used to sample the incoming light. This is represented in Equations 4 and 10 as D.

Sensitivity – The formula for focal spot radius is:

$$\rho = \frac{f\lambda}{D} \qquad \text{Equation 4.}$$

The formula for the number of pixels across the diameter of a focal spot is:

$$n_{px} = \frac{2\rho}{p_x} \qquad \text{Equation 5.}$$

where ρ is the radius or focal spot half-width, f is the lenslet focal length, D is diameter of the lenslet, λ is the light wavelength, p is the pixel width, and n is the number of pixels across the focal spot.

Sensitivity (or resolution) is related to the minimum measurable shift of the focal spot position in the image plane of the wavefront sensor. The focal spot for each lenslet is fairly large, covering several pixels. This provides the Centroid algorithm of Equation 1 with a fairly large sample base, typically 50-100 pixels. Thus pixel noise effects are reduced through averaging, and a very accurate measure of the Centroid can be deduced. Sensor noise and lenslet-to-lenslet optical cross-talk, in our previous experience, limited centroiding accuracy to about 1/100 of a pixel element. Lenslet design and the algorithms have been recently improved so this may now be a conservative estimate for the Centroid accuracy. From Equation 2 the minimum measurable wavefront slope, $(\partial\varphi/\partial x)_{min}$, can be calculated as

$$\frac{\partial\varphi}{\partial x} = \frac{p_x}{(100f)} \qquad \text{Equation 6.}$$

Note that this assumes square camera pixels. This minimum measurable slope is often referred to as the sensitivity or resolution of the instrument, since it represents the minimum resolvable measurement that can be made. For a Shack-Hartmann sensor, it is also the same as the precision or repeatability, since successive measurements will yield different noise realizations whose average is still limited to about 1/100 pixel.

In practice we have found that a good rule of thumb for the minimum measurable peak-to-valley wavefront over the whole aperture can be expressed as

$$\varphi_{min} \approx \sqrt{N_{samples}} \cdot \left(\frac{\partial \varphi}{\partial x} \right)_{min} \qquad \text{Equation 7.}$$

This peak-to-valley value may be interpreted as the predicted minimum measurable Sag across a spherical wavefront. Sag is defined[3] as

$$Sag = 1/2[y^2/R] \qquad \text{Equation 8.}$$

where y is the measurement aperture size and R is the radius of curvature for the spherical wavefront. By combining equations 6, 7, and 8 we obtain Equation 9 as a rule-of-thumb formula for maximum detectable radius-of-curvature

$$R_{max} \approx \frac{50 y^2 f}{\sqrt{N_{samples}} \cdot p_x} \qquad \text{Equation 9.}$$

Dynamic Range – The largest wavefront slope the sensor can measure, or dynamic range, is limited in several ways. Clearly, when adjacent focal spots collide, no meaningful measurement can be made. However, the Centroid algorithm works only over a small region of interest that is usually defined when the reference image is stored. If the focal spot wanders outside this region of interest, then inaccurate Centroid values will result. There are ways to extend this range by tracking the location of the region of interest, but this is usually too complicated for normal operation. The size of these regions of interest is (for a collimated reference) just the distance between the focal spots D. Thus the dynamic range is simply

$$\theta_{max} = \frac{D}{2f} \qquad \text{Equation 10.}$$

Resizing Optics
Two primary functions exist for the resizing optics: 1) Adapting the measurement aperture size to the wavefront sensor aperture, and 2) Imaging the test object onto the wavefront sensor array. Wavefront Sciences manufactures a number of Off-the-Shelf resizing options for each wavefront sensor. Figure 4 shows a typical resizing optical system. Note the point-to-point reimaging illustrated by the dotted rays.

1) The measurement aperture size is adapted to the wavefront sensor aperture by building an optical system with a magnification to provide the beam scaling.
2) The test object's principle plane is imaged onto the wavefront sensor lenslet array by positioning both the test optic and the wavefront sensor at the conjugate planes for the resizing optical system. This means that every point on the test optic maps to a single point on the wavefront sensor.
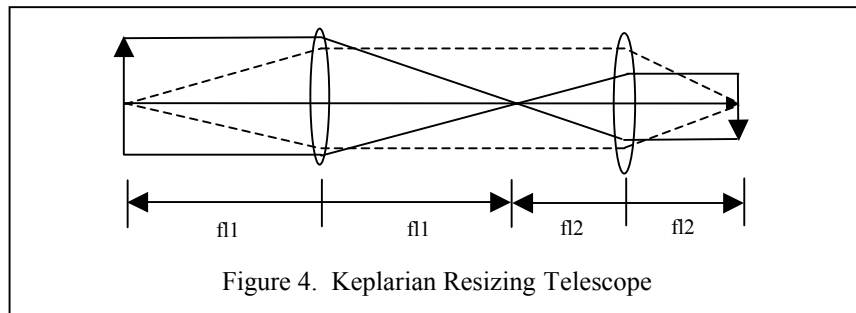

Figure 4. Keplarian Resizing Telescope

Example Application

The design method described above was applied to an example instrument intended to measure intraocular lenses (IOL's). The principle behind the IOL tester is that a
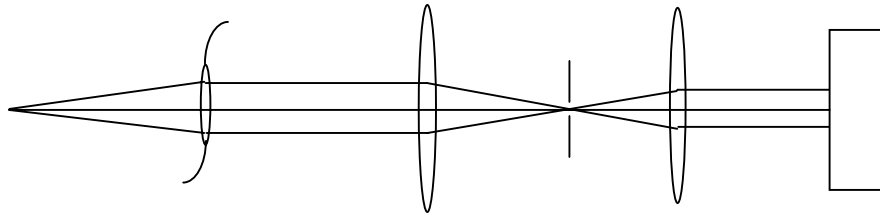

Figure 5. IOL Aberrometer Instrument

point light source is collimated by the test optic. The wavefront sensor is used during the measurement cycle to detect the degree of collimation and provide data to move the point source back and forth in a closed feedback loop. Once the light source is located at the at the optimum collimation point, a position digitizer reads the distance of the point source from the principle plane of the test optic. The inverse of this distance is then reported as the focal power of the lens. The higher order aberrations are measured from a polynomial fit to the wavefront sensor measurement. This configuration was chosen because it allows for the large dynamic range required by the IOL measurement. Several patents are relevant to the use of this technique in a commercial instrument including Patent 5,936,720 and 6,130,419. Other patents are pending.

Test Object – Intraocular Lenses (IOL's) are manmade lens used to replace the human eye's crystalline lens

Figure 6. Haptic IOL Lens

after removal during cataract surgery[4]. Many materials are now available for the manufacture of these lenses. Two of the most common materials are made of PolyMethylMethaAcrylate (PMMA) with an index of refraction of 1.4912 at 20° C or silicone with an index of refraction of 1.4128 at 20° C. The index of refraction of the material may change considerably with temperature[5]. Typical lens diameter is 7.0 mm. The optical zone usually measured and discussed is 5.0 mm. For the purpose of this paper we tested only a single IOL geometry. These lenses are called Haptic IOL's by the vision industry and have mounting whiskers or s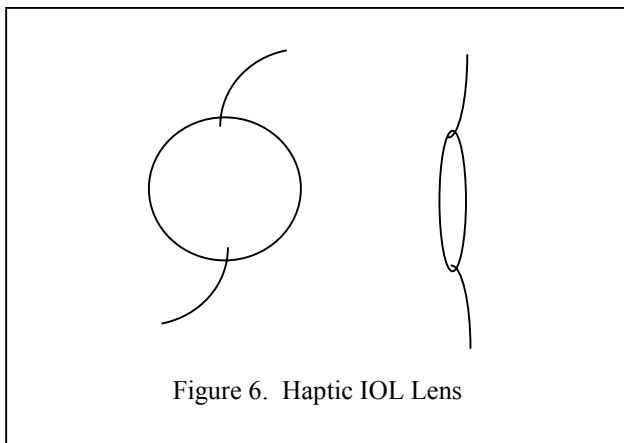prings imbedded in the lens material as shown in Figure 6. Many other geometries are available and will be accommodated by providing interchangeable inserts for the mounting fixture. The focal lengths of these optics range from 200 mm (5 diopters) to 25 mm (40 diopters).

Because it is necessary to measure the optics in a wet environment we may use Equation 11 to convert the power in air to power in water.

$$P_{water} = P_{air} \frac{n_{lens} - n_{water}}{n_{lens} - 1}$$
  Equation 11.

where P_{water} is the power of the lens in diopters (inverse of the focal length) as measured under water, P_{air} is the power in air, n_{water} is the index of refraction of water (assumed to be 1.331456). and n_{lens} is the index of refraction of the lens under test. This number is unique to each optic manufacturer.

Light Source – Experiments for this paper were done using a 635 nm fiber coupled laser diode source from Thorlabs. The production instrument will use a fiber coupled laser diode at 530 nm. This wavelength is near where the human eye is most sensitive and so most vision corrective optics are designed for that wavelength. The power of this source will be capable of being controlled by the data acquisition computer.

Wavefront Sensor – The wavefront sensor chosen for the prototype instrument was based on a visible light 10 bit digital CCD camera. This camera has 6.5mm X 4.5mm aperture, and 9.8 μm square pixels. The lenslet array was chosen to be 4.6 mm focal length. The lenslet array size is 58 X 44 lenslets. We can compute the predicted minimum measurable power by taking the reciprocal of the radius-of-curvature from Equation 9. Note – this computation assumes the measurement is made over the whole sensor aperture and does not include the effects of the resizing optics.

<div align="right">Equation 12.</div>

$$Power_{min} \approx \frac{1}{R_{max}} = \frac{\sqrt{n_{samples}} \cdot p_x}{50\, y^2 f} = \frac{\sqrt{58 \cdot 44} \cdot 9.8e-3}{50 \cdot 25 \cdot 4.6} \cdot 1000 \approx 0.09 \; diopters$$

Resizing Optics – In order to adequately map the 7.0 mm diameter of the test optic onto the sensor aperture a 1.33:1 telescope was chosen. This provides a magnification of 0.75 and reduces the 5.00 mm aperture to 3.75 mm.

Photo 1. Production Prototype Optics Tester

3. DATA

Our market research suggested that the IOL tester needed to have an absolute accuracy of 0.125 diopters. The contact lens tester needed to have a wet cell measurement absolute accuracy of 0.05 diopters. The spatial resolution for both instruments needed to be sufficient to measure 5th order aberrations. Three experiments were done to test measurement repeatability, accuracy and spatial resolution. The repeatability experiment was done using the IOL test configuration since this was thought to be the most challenging in terms of actual component placement repeatability. The accuracy and spatial resolution tests were done using a configuration designed to test contact lenses. This measurement had stronger customer requirements for these to performance parameters. The primary difference between the two configurations

were that the contact lens tester used a fixed pre-collimated light source instead of the bare fiber on a stage and the resizing optics consisted of a 2:1 telescope instead of a 1.25:1. This is because contact lenses are larger and have much less power underwater. In both cases the Zernike circle for the polynomial fit was sit to approximately 5 mm. The same wavefront sensor was used to demonstrate feasibility of the contact lens tester even though we planned to use a higher sensitivity camera for the actual instrument. This was due to budget and scheduling considerations for this study.
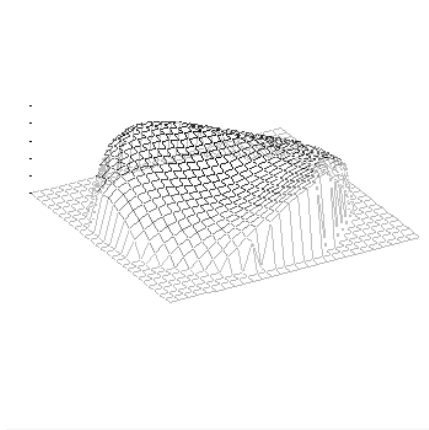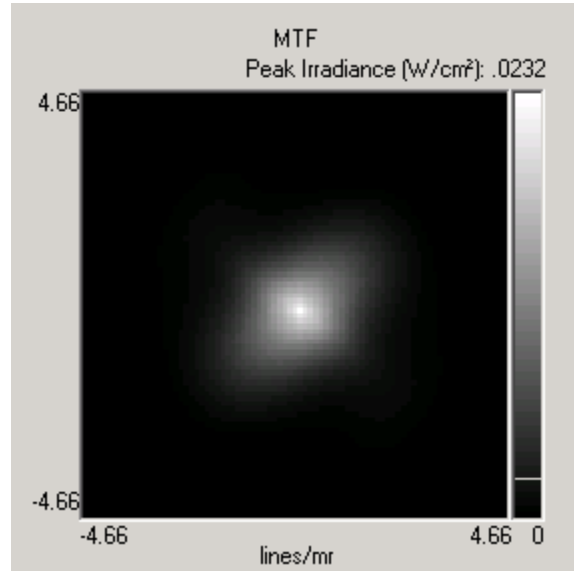

Figure 7. Typical IOL Phase Map

Figure 8. Typical IOL MTF

Repeatability

Effective Power was measured for four different Silicone IOL's from various manufacturers. The manufacture's reported Power for each lens was 20 diopters. Each lens was measured 11 times. In between measurements, the lenses were removed and rotated 180° and then replaced in the fixture. Table 2 summarizes the measurements.

Lens	Effective Power	Standard Deviation
A	19.89 diopters	0.06
B	19.86 diopters	0.06
C	20.23 diopters	0.03
D	20.11 diopters	0.19

Table 2. Repeatability Data

The standard deviation was larger than expected for Lens D, so we investigated further. It had been noted the room temperature fluctuated considerably during this measurement, as the air conditioning had just been turned on for the year and was not yet adjusted properly. At the beginning of the measurements the temperature was noted to be 75° F and was 83° F by the end of the sequence. It was hypothesized that the change in temperature might account for the change in focal power. It is noted in the literature that a positive change in temperature results in a negative change in focal power[5]. This is due to a change in index of refraction of the lens material.

IOL Measurement Series - Lens C
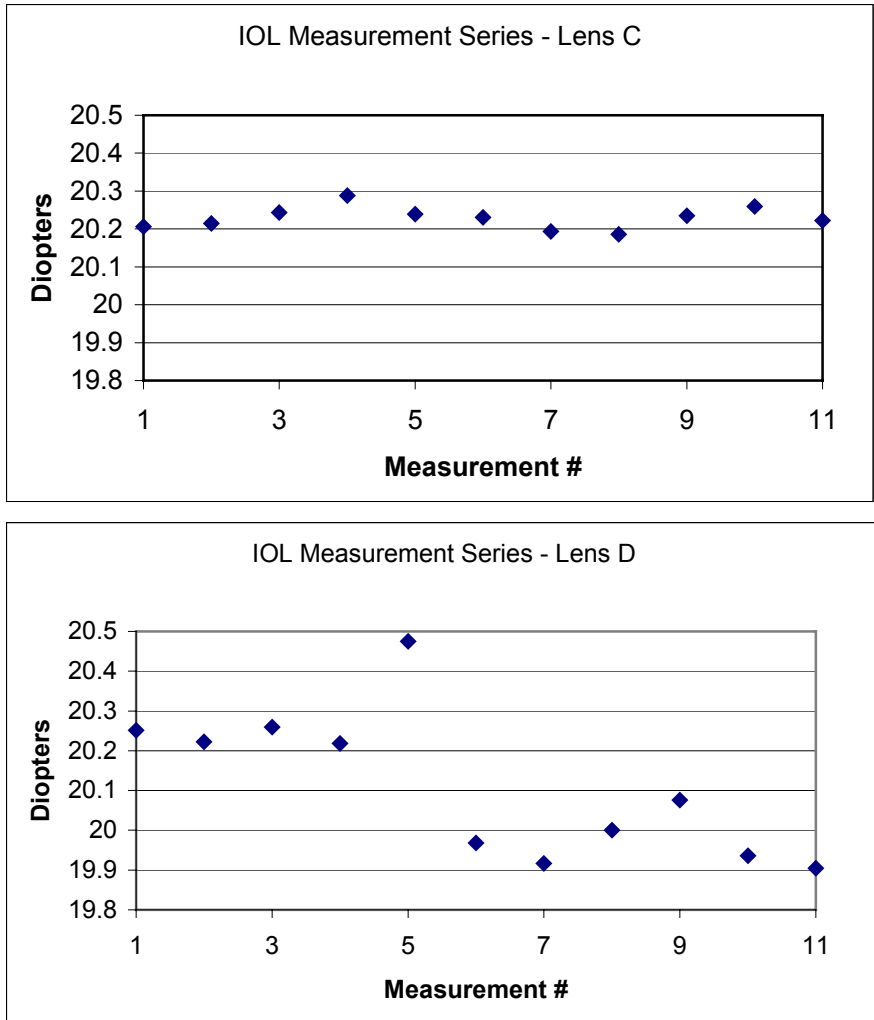

IOL Measurement Series - Lens D

Figure 9. Lens C and D individual measurement data

A plot of the data (Figure 9) shows a definite downward trend for lens D when compared with the data for lens C, which did not show appreciable temperature change. The points are not necessarily equidistant in time. Note that most of the variation comes from a single outlier point. This may have been due to an error in placement of the IOL in the test fixture or the air conditioning system cycling may have caused it. A future experiment will explore temperature effects in greater detail.

Absolute Accuracy

In order to test the absolute accuracy of the aberrometer we needed a lens with known power to use as a test standard. This lens needed to be of appropriate size and testable in the same wet environment as the target optics. For these purposes we chose a 0.5 inch uncoated singlet made by Newport Inc, part number BK7. The manufacturer specifies the Index of Refraction as 1.515014 and the focal length as 250 mm. We performed a Focault Knife Edge Test and obtained 250.39 mm as the focal length or 3.99 diopters. Applying Equation 11 gives us a power of 1.42 diopters in the wet cell. After measuring the lens with the aberrometer we obtained a focal length measurement of 718 mm in the wet cell or 1.39 diopters. The difference yields an absolute error of 0.03 diopters.

Spatial Resolution

A phase plate was manufactured to have pure Z(5,5) aberration. This phase plate was measured with the aberrometer in the contact lens configuration. The resulting phase map is shown in Figure 10. The same

phase plate was measured with a Zygo interferometer in a "dry" configuration as shown in Figure 11. The measurements may not be compared quantitatively since the material changes Refractive Index rapidly when exposed to air and the Zygo setup was not designed to measure the optic in the required wet environment. Note that the two instruments present the data with opposite sign conventions. This test demonstrates that the Shack-Hartmann aberrometer is capable of the required spatial resolution.
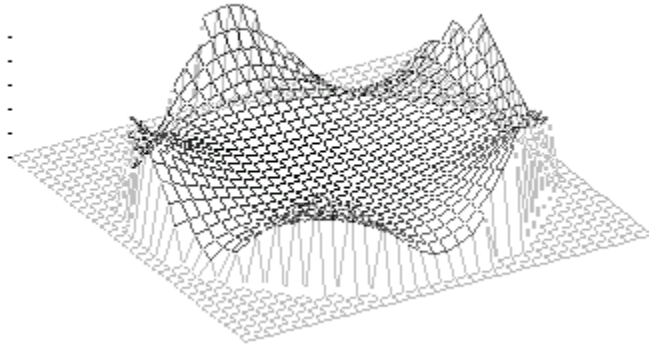

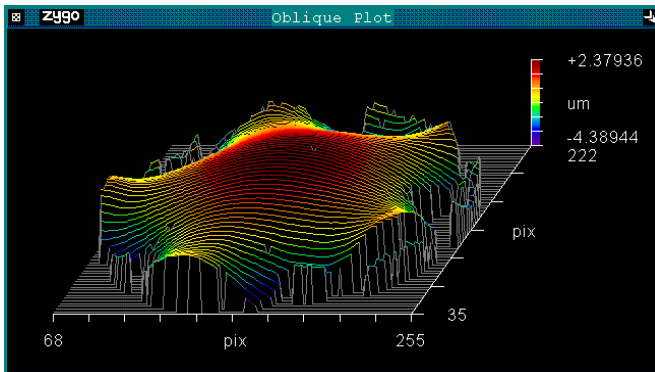
Figure 10. Aberrometer Phase Map

Figure 11. Zygo Interferometer Phase Map

4. CONCLUSIONS

The tests show that the aberrometer as designed can meet the repeatability requirements for Intraocular lens testing if proper attention is paid to temperature and optic placement control. In practice we were able to achieve a better accuracy for the contact lens test instrument than was predicted in our original model. As more data becomes available we may be able to make Equation 6 a little less conservative. In order to meet the absolute accuracy requirements for multi-zonal contact lens testing it was determined that a higher resolution (smaller pixel) camera will be required. The production instrument will use a 1004 X 1004 pixel, 10 bit, digital camera with a pixel size of 7.4 μm.

REFERENCES

1. D. R. Neal, R. J. Copland, J. Roller, "Shack-Hartmann Wavefront sensor precision and accuracy," Advanced Characterization Techniques for Optical, Semiconductor, and Data Storage Components, SPIE Volume 4779, 2002.
2. D. R. Neal, D. J. Armstrong, and W. T. Turner, "Wavefront Sensors for Control and Process Monitoring in Optics Manufacture," Lasers as Tools for Manufacturing II, SPIE Volume 2993, 1997.
3. J. M. Geary, "Introduction to Wavefront Sensors," pp 42, SPIE – The International Society for Optical Engineering, 1995.

4.   H. V. Gimbel, and E. E. Anderson Penno, "Chapter 9.   Refractive Lensectomy," pp 160-169 and "Chapter 13.   Phakic Intraocular Lenses," Refractive Surgery: A Manual of Principles and Practice, pp 199-229, SLACK Incorporated, 2000.

5. J. T. Holladay, S. V. Gent, A. C. Ting, V. P. Portney, and T. R. Willis, "Silicone Intraocular Lens Power vs Temperature, Ophthalmology," Vol 107, No. 4, April 1989.